Protein Engineering, Design & Selection vol. 18 no. 9 pp. 425–433, 2005
Published online August 10, 2005 doi:10.1093/protein/gzi051

How to improve nature: study of the electrostatic properties of the surface of α-lactalbumin

Serge E.Permyakov[1], George I.Makhatadze[2], Rikard Owenius[3], Vladimir N.Uversky[1,4,5], Charles L.Brooks[6], Eugene A.Permyakov[1] and Lawrence J.Berliner[3]

[1]Institute for Biological Instrumentation, Russian Academy of Sciences, Pushchino, Moscow Region, Russia, [2]Department of Biochemistry and Molecular Biology, Penn State University, College of Medicine, Hershey, PA 17033, [3]Department of Chemistry and Biochemistry, University of Denver, Denver, CO 80208, [4]Center for Computational Biology and Bioinformatics, Department of Biochemistry and Molecular Biology, School of Medicine, Indiana University – Purdue University, Indianapolis, IN 46202 and [6]Department of Veterinary Biosciences, The Ohio State University, Columbus, OH 43210, USA

[5]To whom correspondence should be addressed.
E-mail: vuversky@iupui.edu

It was recently shown that α-lactalbumin interacts with histones and simple models of histone proteins such as positively charged polyamino acids, suggesting that some fundamental aspects of the protein surface electrostatics may come into play. In the present work, the energies of charge–charge interaction in apo- and Ca^{2+}-loaded α-lactalbumin were calculated using a Tanford–Kirkwood algorithm with either solvent accessibility correction or using a finite difference Poisson–Boltzmann method. The analysis revealed two major regions of α-lactalbumin that possessed highly unfavorable electrostatic potentials: (a) the Ca^{2+}-binding loop and its neighboring residues and (b) the N-terminal region of the protein. Several individual mutants were prepared to neutralize specific individual surface acidic amino acids at both the N-terminus and Ca^{2+}-binding loop of bovine α-lactalbumin. These mutants were characterized by intrinsic fluorescence, differential scanning microcalorimetry and circular dichroism. The structural and thermodynamic data agree in every case with the theoretical predictions, confirming that the N-terminal region is very sensitive to changes in charge. For example, desMet D14N mutation destabilizes protein and decreases its calcium affinity. On the other hand, desMet E1M and desMet D37N substitutions increase the thermal stability and calcium affinity. The Met E1Q is characterized by a marked increase in protein stability, whereas desMet E7Q and desMet E11L display a slight increase in calcium affinity and thermal stability. Examination of the unfavorable energy contributed by Glu1 and the energetically favorable consequences of neutralizing this residue suggests that nature may have made an error with bovine α-lactalbumin from the viewpoint of stabilizing structure and conformation.

Keywords: α-lactalbumin/calcium binding/electrostatic interactions/site-directed mutagenesis/thermal stability

Introduction

α-Lactalbumin (α-LA) is a small (14 kDa), highly abundant calcium-binding protein from milk, which has, after decades of intensive study, become one of the best characterized proteins in protein science [for a review, see Permyakov and Berliner (2000)]. One of the reasons for the high interest in α-LA is its ability to convert under mild denaturing conditions into the equilibrium molten globule state, representing what is now considered a general intermediate in protein folding (Dolgikh *et al*., 1981). Recently, several reports have uncovered bactericidal and antitumor activities of α-LA and its fragments. For example, Pellegrini *et al*. and colleagues have found that proteolytic digestion of α-LA yields three peptides with bactericidal properties (Pellegrini *et al*., 1999). Hakansson *et al*. have established that a multimeric form of human α-LA derivative (MAL) isolated from the casein fraction of milk is a potent apoptosis-inducing agent with broad, yet selective, cytotoxic activity (Hakansson *et al*., 1995). MAL was shown to kill all transformed, embryonic and lymphoid cells tested, but spared mature cells. It was shown that the apoptosis-inducing fraction contained α-LA oligomers that underwent a conformational change toward a molten globule-like state (Svensson *et al*., 1999). MAL crosses the plasma membrane and enters the nucleus where it induces DNA fragmentation through some direct effect at the nuclear level (Hakansson *et al*., 1999).

Similar results were obtained with HAMLET (human α-LA made lethal to tumor cells) or BAMLET (bovine α-LA made lethal to tumor cells), which is native α-LA converted *in vitro* to an apoptosis-inducing form of the protein when in a stoichiometric complex with oleic acid (Svensson *et al*., 1999, 2000). HAMLET was shown to trigger apoptosis in tumor and immature cells, but healthy cells were resistant. HAMLET passed through the cytoplasm to the nucleus and accumulated in the cell nucleus. In tumor cells *in vivo*, HAMLET co-localized with histones and perturbed the chromatin structure (Duringer *et al*., 2003). HAMLET was found to bind histone HIII strongly and to lesser extent histones HIV and HIIB. The binding of histones by HAMLET impaired their interaction with DNA. Based on these observations, it was concluded that HAMLET interacts with histones and chromatin in tumor cell nuclei, locking the cells into the apoptotic pathway via an irreversible disruption of chromatin organization (Duringer *et al*., 2003).

Recently, it was found that non-fatty acid-bound monomeric bovine and human α-LAs interacted electrostatically with basic proteins, histones and positively charged polyamino acids as simple models of histone proteins (Permyakov *et al*., 2004). Thus, complexation of α-LA with oleic acid is not required for the interaction with histone proteins. The intrinsic ability of α-LA to interact strongly with charged polymers suggests that the protein surface possesses some electrostatic properties which complement this interaction.

Mutations of surface charged residues in multi-subunit proteins can increase their stability. For example, mutation of Glu165 to Gln or Lys in tetrameric malate dehydrogenase

caused a dramatic increase in thermal stability at pH 7.5 (increase by about 24°C) (Bjork *et al*., 2004). Remarkably, the crystal structures of the two mutants showed only minor structural changes localized in close proximity to the mutated residues, indicating that the observed stability changes were caused by subtle changes in the complex network of electrostatic interactions at the dimer–dimer interface.

Minagawa *et al*. constructed a thermostable mutant of lactate oxidase (Minagawa *et al*., 2003). Their molecular modeling suggested that the substitution of Gly for Glu at position 160 reduced the electrostatic repulsion between the negative charges of Glu160 and Glu130 in the $(\beta/\alpha)_8$ barrel structure, but thermal inactivation experiments on the five different single-mutant lactate oxidases at position 160 (E160A, E160Q, E160H, E160R and E160K) showed that it was the side-chain molecular volume of the residue at position 160 that was the primary contribution to the thermostability.

Protein engineering experiments on glycosyl hydrolase showed that the thermostabilization resulted as a consequence of numerous favorable ionic interactions in the 83–124 sequence with the other parts of protein matrix that became more rigid and less accessible to thermally activated solvent molecules (Bismuto *et al*., 2003).

Seven hyper-stable multiple mutants of staphylococcal nuclease have been constructed by various combinations of eight different stabilizing single mutants (including mutations of negatively charged residues—D21N and D21K) (Chen *et al*., 2000). Their thermal denaturation midpoint temperatures were 12.6–22.9°C higher than that of the wild-type. The crystal structures of these mutants were solved at high resolution, yet no major structural changes were found, with most changes localized around the site of mutation. Rearrangements were observed in the packing of side chains in the major hydrophobic core, although none of the mutations were in the core. Surprisingly, detailed structural analysis showed that packing had improved, with the volume of the mutant hydrophobic core decreasing as protein stability increased. The authors believed that these results indicate that optimization of packing follows as a natural consequence of increased protein thermal stability and that good packing is not necessarily the proximate cause of high stability (Chen *et al*., 2000). The mutants showed that increased numbers of electrostatic and hydrogen bonding interactions are not obligatory for large increases in protein stability. Based on the electrostatic energy calculations, it has been suggested that at least two of mutants, D21N and D21K, increase stability by removing unfavorable electrostatic interactions (Chen *et al*., 2000).

The development of reliable methods for the prediction of result of mutations in protein requires the knowledge of the force field. This is a complex task that should take into account the delicate balance between the different energy terms that contribute to protein stability. The force fields usually use an effective physical energy function or they are based on statistical potentials where energies are derived from the frequency of residue or atom contacts in the protein database or they use empirical data obtained from experiments. For example, a computer algorithm, FOLDEF (for FOLD-X energy function), has been developed to provide a fast and quantitative estimation of the importance of the interactions contributing to the stability of proteins and protein complexes (Guerois *et al*., 2002). At the same time, the free energy of protein unfolding includes several contributions, some of which are difficult to estimate. For this reason, the predictive power of methods developed so far is still not as high as desired and researchers continue to suggest new approaches. Mozo-Villarias *et al*. have developed a thermostability criterion for a protein in terms of a quasi-electric dipole moment (contributed by its charged residues) defined for an electric charge distribution whose total charge is not zero (Mozo-Villarias *et al*., 2003). It was found that minimization of the modulus of this dipole moment increased its thermal stability. In spite of these efforts to create methods for prediction of effects of mutations on stability of proteins, we still do not have reliable and simple approaches to solve this problem.

In the work presented here, the energies of charge–charge interactions in apo- and Ca^{2+}-loaded α-LA were calculated using a Tanford–Kirkwood algorithm with solvent accessibility correction or using the finite difference Poisson–Boltzmann method. These continuum electrostatic models have been shown to capture successfully the interactions between ionizable residues on the protein surfaces (for reviews, see Klapper *et al*., 1986; Gilson, 1995; Elcock and McCammon, 1998; Schaefer *et al*., 1998; Schutz and Warshel, 2001; Dong and Zhou, 2002; Bashford, 2004; Dominy *et al*., 2004; Feig *et al*., 2004; Garcia-Moreno and Fitch, 2004). The analysis revealed that several residues in the α-LA sequence have unfavorable charge–charge interactions. The theoretical predictions were confirmed by site-directed mutagenesis of those charged surface residues and detailed physico-chemical characterization of each mutant protein. The experimental data obtained were in good qualitative agreement with the theoretical predictions.

Materials and methods

Materials

Bovine α-LA (lot 60K7002) was purchased from Sigma Chemical (St. Louis, MO) and used without further purification. Protein concentrations were determined spectrophotometrically using an extinction coefficient $E_{1\%,\ 280\ nm} = 20.1$ (Kronman *et al*., 1964). EDTA standard solutions (Fisher Scientific) were used for calcium titration. All other chemicals were of reagent grade or higher. All solutions were prepared with distilled, deionized water.

Recombinant proteins were prepared as described previously (Anderson *et al*., 1997). The mutant plasmids were prepared by the method of Kunkel (Kunkel, 1985). All proteins were characterized by absorption, fluorescence and CD spectroscopy.

All of the recombinant α-LAs retained the additional N-terminal methionine residue which was previously found to contribute to both decreased thermal stability and lower calcium affinity (Ishikawa *et al*., 1998; Chaudhuri *et al*., 1999; Veprintsev *et al*., 1999). Selective removal of the N-terminal Met was achieved using *Aeromonas proteolitica* aminopeptidase (Wilkes *et al*., 1973; Prescott and Wilkes, 1976) as described by Veprintsev *et al*. (1999). Only the amino terminal Met is removed as the activity of this aminopeptidase is stopped by N-terminal amino acids with large negatively charged side chain (i.e. the first residue, Glu1, in the native bovine α-LA sequence). Briefly, the digestion reaction was performed at a substrate to enzyme ratio of about 100:1 (α-LA ≈ 2 mg/ml, 2 h, 37°C, 10 mM HEPES,

pH 8.0). Excess EDTA (final concentration, 10 mM) was added to quench the reaction. Proteins were separated by gel filtration on a Sephadex G-100 column and fractions containing α-LA were collected, dialyzed against 10 mM ammonium bicarbonate and lyophilized.

Saturation of intact and mutant α-LA by calcium ions was achieved via addition of 1 mM $CaCl_2$. The use of higher concentrations of calcium could result in saturation of the weaker secondary calcium-binding site of α-LA (Aramini *et al*., 1992). Removal of Ca^{2+} was achieved via addition of 1 mM EDTA. Higher concentrations of EDTA could promote EDTA binding to α-LA (Permyakov *et al*., 1987).

Instrumentation and methods

Fluorescence measurements. Fluorescence measurements were performed on a Perkin-Elmer LS50B or a laboratory-made instrument with a precision titrator device and Peltier temperature-controlled cell holder described previously (Permyakov *et al*., 1977). The excitation wavelength was 280.4 nm. All spectra were corrected and fit to log-normal curves using non-linear regression analysis (Marquardt, 1963) to obtain the emission maximum for each spectrum (Burstein and Emelyanenko, 1996). In all fluorescence experiments, illumination time and UV irradiation power levels were minimized in order to avoid UV-induced structural rearrangements (Vanhooren *et al*., 2002; Permyakov *et al*., 2003).

Temperature scans were performed stepwise, allowing the sample to equilibrate at each temperature for at least 5 min. Temperature was monitored directly inside the cell. The fraction of conversion from the native to the thermally unfolded state was calculated as described previously (Permyakov and Burstein, 1984; Permyakov, 1993).

The calcium binding affinity of each α-LA mutant was measured by spectrofluorimetric back-titration of the calcium-loaded protein with a strong calcium chelator (e.g. EDTA) at fixed pH. Calculations of the calcium association constant from the experimental data were based on a competitive binding scheme between protein (P) and chelator (H) for calcium ions (Permyakov *et al*., 1985; Permyakov, 1993):

$$\begin{aligned} P + Ca^{2+} &\overset{K_1}{\longleftrightarrow} P \cdot Ca^{2+} \\ H + Ca^{2+} &\overset{K_2}{\longleftrightarrow} H \cdot Ca^{2+} \end{aligned} \tag{1}$$

where K_1 and K_2 correspond to protein and chelator calcium equilibrium association constants, respectively. The value of K_1 was estimated using non-linear regression analysis (Marquardt, 1963) based upon K_2 values from Schwarzenbach and Flaschka (1965).

Calcium binding and protein stability. The role of calcium on stability is linked to the difference in binding affinity for the folded protein and the unfolded protein (Permyakov *et al*., 1985):

$$\begin{array}{ccc} U & \leftrightarrow & F \\ \updownarrow & & \updownarrow \\ U_{Ca} & \leftrightarrow & F_{Ca} \end{array} \tag{2}$$

where U and U_{Ca} correspond to the calcium-free and calcium-loaded unfolded states, and F and F_{Ca} correspond to the calcium-free and calcium-loaded native states. If the two horizontal equilibria are described by free-energy differences $-\Delta G_0$ and $-\Delta G_1$ and the two vertical equilibria by binding constants K_0 and K_1, respectively, then the thermodynamic cycle results in the rigorous relation

$$\Delta G_1 - \Delta G_0 = RT\ln(K_1/K_0) \tag{3}$$

Because calcium has a much higher affinity for the folded state (i.e. $K_1 \gg K_0$), the folding equilibrium of the calcium-loaded state is shifted towards higher temperatures (i.e. $\Delta G_1 \gg \Delta G_0$).

In principle, in the presence of calcium, the total concentration of the folded protein is the sum of the two species, [F] and [F_{Ca}] and similarly for the unfolded state, [U] and [U_{Ca}]. Thus, the overall equilibrium constant can be described as

$$\begin{aligned} \exp(\Delta G/RT) &= ([F] + [F_{Ca}])/([U] + [U_{Ca}]) \\ &= ([F] + K_1[F][Ca])/([U] + K_0[U][Ca]) \\ &= ([F]/[U])(1 + K_1[Ca])/(1 + K_0[Ca]) \\ &= \exp(\Delta G_0/RT)(1 + K_1[Ca])/(1 + K_0[Ca]) \end{aligned} \tag{4}$$

This means that the overall folding equilibrium depends on calcium concentration. Furthermore, as follows from Equation 4, the addition of a strong calcium chelator (such as EDTA/EGTA) will decrease the free calcium concentration, shifting the chemical equilibrium to the single equilibrium between native and denatured states of apo-protein. Similarly, the saturation of the system by calcium will result in a single equilibrium between native and denatured states of the calcium-bound protein. That is why the addition of 1 mM EDTA or 1 mM $CaCl_2$ was used to achieve full calcium depletion or saturation of the system, respectively. Unfortunately, we could not use higher concentrations of EDTA owing to the possibility of EDTA binding to α-LA (Permyakov *et al*., 1987). Likewise, the use of higher concentrations of calcium may result in saturation of the weaker secondary calcium-binding site of α-LA (Aramini *et al*., 1992).

Scanning calorimetry. Scanning calorimetric measurements were carried out on a VP-DSC differential scanning microcalorimeter (Microcal, Northhampton, MA) at a 0.5 K/min or 1 K/min heating rate in 10 mM HEPES–KOH buffer, pH 7.7. A pressure of 30 psi was maintained in order to prevent degassing of the solutions during heating. Protein concentrations were 0.3–1 mg/ml. The heat sorption curves were baseline corrected. Protein specific heat capacity (C_p) was calculated as described by Privalov and Potekhin (1986). The partial molar volume was calculated according to Hakel *et al*. (1999). The temperature dependence of C_p was fitted to a simple two-state model, assuming that the difference between heat capacities of the denatured and native proteins (ΔC_p) was independent of temperature (all values were normalized by molecular weight):

$$C_p = C_{p,D} - \Delta C_p/(1+K) + \left[\frac{\Delta H_{VH} + \Delta C_p \cdot (T - T_0)}{T(1+K)}\right]^2 \cdot K/R \tag{5}$$

where

$$K = \exp\left[\frac{\Delta H_{VH} - \Delta C_p \cdot T_0}{R}\left(\frac{1}{T_0} - \frac{1}{T}\right) + \frac{\Delta C_p}{R}\ln\frac{T}{T_0}\right],$$

$R = 8.31/\mathrm{MW}$.

Here $C_{p,D}$ is the specific heat capacity of the denatured protein, linearly extrapolated to the transition region. The fitting parameters, ΔC_p, ΔH_{VH} (van't Hoff's enthalpy of protein denaturation) and T_0 (mid-transition temperature) were estimated with the Origin 5.0 software provided with the MicroCal VP-DSC. The free energy change of thermal denaturation, ΔG, was calculated as follows:

$$\Delta G = \Delta H_{VH}(1 - T/T_0) + \Delta C_p T[1 - (T_0/T) - \ln(T/T_0)] \quad (6)$$

Circular dichroism. Circular dichroism measurements were performed on either an AVIV 62DS, Applied Photophysics PiStar or Jasco J-500A spectropolarimeter. Typical instrument conditions were scan rate 5 nm/min and time constant 8 s. The pathlength was 0.19 mm for the far-UV and 10 mm for the near-UV region. All data were baseline corrected.

Electrostatics calculations. The energies of charge–charge interaction were calculated using a TK-SA procedure, implementation of which is described in detail elsewhere (Ibarra-Molero *et al*., 1999; Loladze *et al*., 1999; Makhatadze *et al*., 2003). Briefly, the energy of pairwise interactions between unit charges was calculated according to a Tanford–Kirkwood algorithm (Tanford and Kirkwood, 1957) with the solvent accessibility correction as proposed by Matthew and Gurd (1986). The mean field approximation was used for calculating the effect of charge–charge interactions on the pK_a of ionizable groups from their model compound values (Asp, 4.0; Glu, 4.5; Lys, 10.5; Arg, 12.0; His, 6.3; Tyr, 10.5; N-terminus, 7.7; C-terminus, 3.6). Calculations were performed on the PDB entries 1F6R (apo-form) and 1F6S (Ca^{2+}-bound form) for bovine α-LA (Chrysina *et al*., 2000). Missing atoms were reconstructed using the default option of the SwissPDB Viewer. Calculations of the charge–charge interactions for each of the six structural subunits in each PDB file were performed and average values were reported. For comparison of native α-LA with the various protein mutants, it was assumed that the charge–charge interactions in the unfolded states of these proteins were similar. The results of TK-SA calculations were also compared with the calculation done using the finite difference Poisson–Boltzmann (FDPB) method as implemented in the UHBD software package (Antosiewicz *et al*., 1994) as described (Fitch *et al*., 2002; Makhatadze *et al*., 2004). Both methods gave qualitatively identical results (see below). In addition, charge–charge interactions in the unfolded state were calculated using a Gaussian chain model as suggested by Zhou (2002a). Because the residues of interest are located on the protein surface and have high (>50%) solvent accessibility, the effects of solvation were not explicitly taken into account.

Results and discussion

Energetics of charge–charge interactions in α-LA

Calculations of the energies of the charge–charge interactions were carried out for three α-LA forms: apo-protein (1F6R), holo-protein (1F6S) and an apo-form based on the 1F6S structure with Ca^{2+} ion excluded from the calculations. Comparison of the results from these calculations (Figure 1) reveals several interesting features:

1. In the apo-form, many acidic side chains have unfavorable charge–charge interactions, with 11 residues (Glu1, Glu7, Glu11, Asp63, Asp64, Asp78, Asp82, Asp83, Asp84, Asp87 and Asp88) possessing significantly unpropitious charge–charge interactions.
2. Minor structural rearrangements accompanying Ca^{2+} binding to α-LA (Chrysina *et al*., 2000) do not lead to any significant changes in energies of charge–charge interactions. This can be seen from comparison of charge–charge interactions calculated for apo-α-LA with the results obtained on Ca^{2+}-bound structure without including Ca^{2+} in the calculations.
3. It is clear that Ca^{2+}-binding has the most pronounced effect on residues directly involved in cation coordination. For each of these three residues, Asp82, Asp87 and Asp88, the charge–charge interaction energy, being large and unfavorable in the apo-form, becomes comparably favorable after Ca^{2+} ion binding. Charge–charge interactions of the other two residues in the Ca^{2+}-binding loop, Asp83 and Asp84, are also significantly affected by Ca^{2+} binding. On the other hand, Ca^{2+} binding only slightly affects residues more distant from the Ca^{2+}-binding site and the energy contributions from Glu1, Glu7, Glu11, Asp63 and Asp64, which have large, unfavorable charge–charge interactions in the apo-form, remained essentially unchanged in the Ca^{2+}-bound form.

It is also remarkable that both TK-SA and FDPB/UHBD calculations give qualitatively similar results (Figure 1) despite the differences in the assumptions each model incorporates. In both treatments of energetics of charge–charge interactions it is assumed that the contribution of the residual charge–charge interactions in the unfolded state is small and should not affect qualitatively the results of the calculations. This can be seen from the comparison of the results of FDPB/UHBD calculations for the native state with the calculations done using a Gaussian model of the unfolded chain proposed by Zhou (2002a). It is clear that in the case of α-LA charge–charge interactions in the unfolded state are relatively small and hence justify the assumption that in a qualitative approximation the mutations have an effect only on the charge–charge interactions in the native state.

Based on these observations, one can predict that mutations, which neutralize side chains that are involved in unfavorable charge–charge interactions (e.g. Glu1, Glu7, Glu11), should result in an *increase* in protein stability. Conversely, substitutions leading to charge neutralization on side chains that provide favorable charge–charge interactions (i.e. Asp14, Glu25) should result in a *decrease* in protein stability relative to the native protein. Furthermore, from the analysis presented above, the most dramatic changes would be expected from mutations in the calcium-binding loop (including those non-coordinating residues) and secondly the N-terminal region of the protein.

The energies calculated for the calcium loop were not unexpected and the pronounced stabilization of the apo-form by Ca^{2+} binding originated from the negative charge 'compensation' in the coordination site was demonstrated earlier (Permyakov *et al*., 2001). Until recently, however, the N-terminal region of α-LA had not been examined with respect to charged amino acid residues and protein stability. Consequently, we constructed a set of mutants covering this region in the 3-D structure of α-LA: E1Q, E7Q, E11L, D14N, D37N, including two additional mutants previously reported: ΔE1 (E1M) and E25A (Veprintsev *et al*., 1999; Permyakov

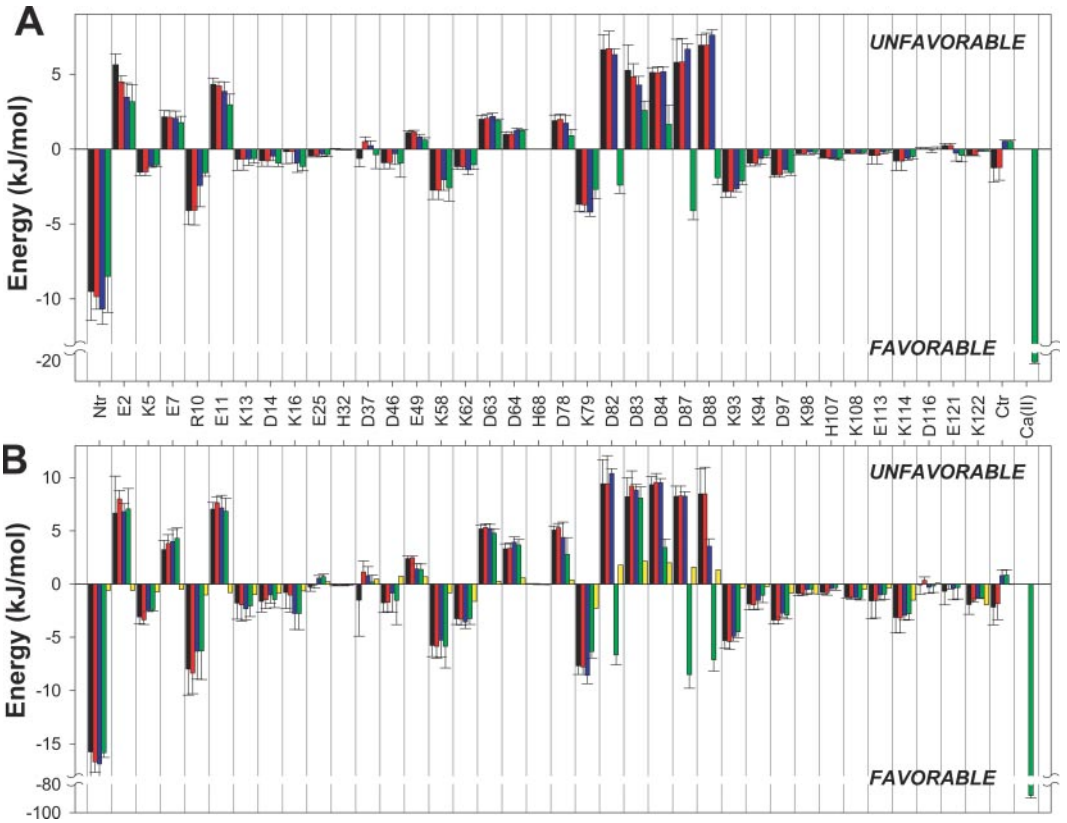

Fig. 1. Comparison of the energies of the charge–charge interactions in bovine α-LA as calculated according to the Tanford–Kirkwood algorithm with the solvent accessibility correction (**A**) and by Finite Difference Poisson–Boltzmann model as implemented by UHBD (**B**). α-Lactalbumin apo-form (1F6R entry of PDB), black bars; holo-form (1F6S structure), green bars; apo-form based on 1F6S structure, red bars, apo-form with additional N-terminal Met modeled into 1F6R structure, blue bars. Yellow bars in (B) show the energetics of charge–charge interactions in the unfolded state calculated using Gaussian chain model (Zhou, 2002a). Each bar represents an average of calculations using six individual models in the PDB (A, B, C, D, E, F) with the errors calculated as standard deviation of the mean.

et al., 2000). Since recombinant α-LA contains an extra methionine residue at the N-terminus, which was found to destabilize protein structure, thermal stability and calcium affinity (Ishikawa *et al*., 1998; Chaudhuri *et al*., 1999; Veprintsev *et al*., 1999), selective removal of the additional N-terminal Met from recombinant proteins was performed using *A.proteolitica* aminopeptidase enzyme [with the exception of the mutants ΔE1 (E1M) and E1Q].

Physico-chemical properties of α-lactalbumin mutants and comparisons with electrostatic calculations

The correctness of folding of α-LA mutants is assessed, in part, from the maximum wavelength positions of the intrinsic fluorescence spectra (λ_{max}) of Ca^{2+}-loaded (1 mM $CaCl_2$) α-LA forms (see Table I). This spectral parameter reflects the mobility and polarity of the environment of emitting residues in proteins and generally reflects the degree of accessibility to solvent molecules (Permyakov, 1993). All of the mutants studied here, except for desMet E25A, possess similar λ_{max} values, within 4–5 nm, which indicates only slight structural perturbations of the environment of their tryptophan residues. The increase of 8–9 nm in λ_{max} for desMetE25A α-LA reflects a significantly increased Trp exposure to solvent compared with native α-LA.

The far-UV circular dichroism analyses suggest a high α-helical content in all of the mutants studied (data not shown), confirming that all retain a native-like α-LA fold.

Typical spectrofluorimetric thermal denaturation curves for the apo- (1 mM EDTA, pH 7.7) and calcium-loaded (1 mM $CaCl_2$) states of desMet-D37N α-LA are shown in Figure 2. A red shift in the λ_{max} value with temperature corresponds to a progressive exposure of Trp residues to solvent water accompanying protein denaturation. It is remarkable that the D37N substitution shifts the thermal unfolding transition toward *higher* temperature, both in the absence and presence of calcium. Similar observations were found from scanning microcalorimetry (Figure 3).

Although very similar thermal transition mid-temperature (t_m) values were extracted from the DSC data, some differences have been found earlier between fluorescence and calorimetric data with apo-α-LA (Veprintsev *et al*., 1997). We report t_m values from the fluorescence experiments here since they were run at significantly lower protein concentrations than required for DSC, which minimizes the possibilities for aggregation and also allows the use of high EDTA:protein ratios in the calcium back-titrations. This was particularly important with mutants exhibiting increased calcium affinity.

Table I summarizes all of the thermal transition mid-temperatures (t_m) for the α-LA species in this work. Every mutant studied possessed a thermal transition, even in the absence of calcium. Hence none of these mutations resulted in a total loss of protein tertiary structure. Yet desMet D14N α-LA displayed the most significant decrease in thermal stability, in both the absence and presence of calcium, resembling recombinant wt α-LA. A similar, but less pronounced, destabilization was observed for desMet E25A α-LA. On the other hand, ΔE1(E1M) and desMet D37N α-LA exhibited significantly increased thermal stabilities (see Table I). Overall, the

Table I. Physico-chemical properties of bovine α-LA mutants from intrinsic fluorescence measurements (pH 7.7, 10 mM HEPES–KOH)

α-Lactalbumin	t_m apo (°C)	t_m Ca^{2+} (°C)	K_{Ca} 45°C (M^{-1})	λ_{max} Ca^{2+}, 5°C (nm)	$\Delta\Delta G_{n\rightarrow m}$ apo (kJ/mol)	$\Delta\Delta G_{n\rightarrow m}$ Ca^{2+} (kJ/mol)
Intact	26.2	67.9	9×10^6	323.3	0	0
Rec. wild type	≪20	59.8	1.1×10^6	320.3	≪–2.5	−7.1
E1Q	23.5	66.6	3.6×10^6	322.9	−1.2	−1.2
DE1 (E1M)	36.8	69.8	52×10^6	324.4	6.2	1.7
desMet E7Q	27.0	67.7	10×10^6	322.0	0.4	–0.2
desMet E11L	27.5	69.5	11×10^6	320.6	0.6	1.5
desMet D14N	≪20	56.8	1.1×10^6	319.8	≪–2.5	–9.6
desMet E25A	19.5	60.9	5×10^6	331.8	–2.7	–6.2
desMet D37N	31.7	74.2	26×10^6	321.3	2.9	5.9

Concentration of calcium ions was controlled by addition of either 1 mM $CaCl_2$ (*Ca^{2+}*) or 1 mM EDTA (*apo*). t_m, mid-transition temperature; K_{Ca}, equilibrium calcium association constant; λ_{max}, emission spectrum maximum position; $\Delta\Delta G_{n\rightarrow m}$, mutation-induced change in the Gibbs free energy of thermal denaturation was estimated from t_m values based on the DSC data for the native protein.

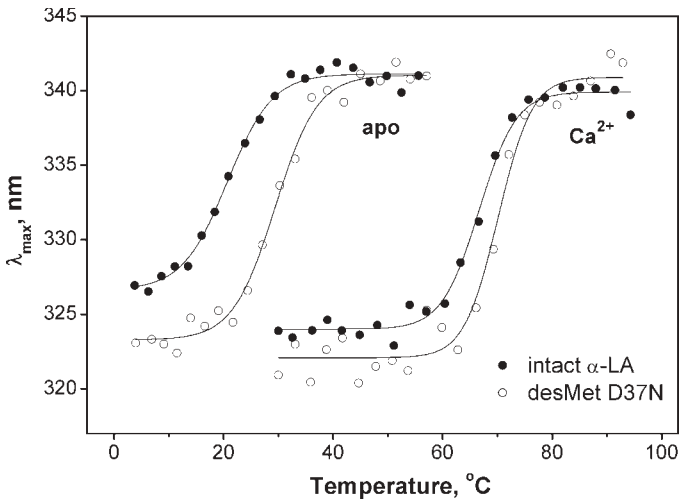

Fig. 2. Comparison of the thermal denaturation profiles of desMet D37N and native α-LA (pH 7.7, 10 mM HEPES–KOH) as monitored by intrinsic fluorescence spectroscopy. Concentration of α-LA was 5–8 μM. Concentration of calcium ions was controlled by addition of either 1 mM $CaCl_2$ (*Ca^{2+}*) or 1 mM EDTA (*apo*). The excitation wavelength was 280.4 nm.

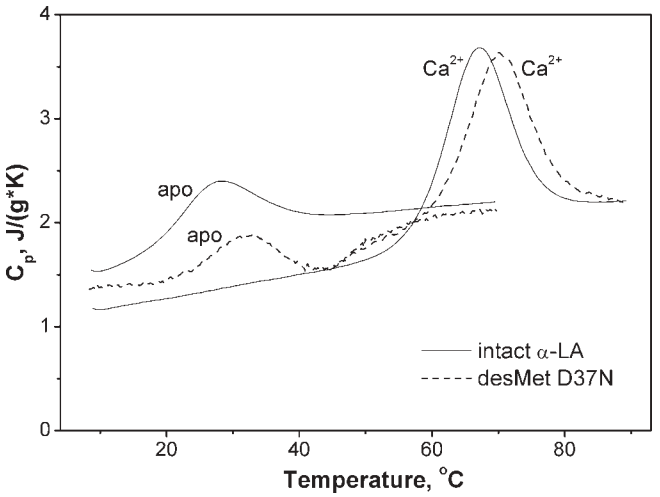

Fig. 3. Comparison of the calorimetric profiles of desMet D37N α-LA and the intact protein (pH 7.7, 10 mM HEPES–KOH). Concentration of α-LA was 0.3–1 mg/ml. Concentration of calcium ions was controlled by addition of either 1 mM $CaCl_2$ (*Ca^{2+}*) or 1 mM EDTA (*apo*). Heating rate was 0.5 or 1 K/min.

charge-neutralizing mutations in the N-terminal region of α-LA resulted in protein forms differing in thermal stability by more than 17°C, suggesting very unusual electrostatic interactions in this region. Yet other substitutions that were predicted to increase thermal stability, namely desMet E7Q and desMet E11L, resulted in relatively minor effects (<2°C).

The results obtained with E1Q α-LA are especially interesting. Although this mutant exhibited slightly lower thermal stability (1–3°C) with respect to native α-LA, this particular mutant contains an additional N-terminal Met residue, thus E1Q α-LA should be compared with recombinant wild-type α-LA. Consequently, removal of the negative charge at Glu1 in wild-type α-LA results in a substantial recovery of protein thermal stability. The same effect was observed for the native protein, i.e. substitution of Glu1 by Met1 in the ΔE1(E1M) mutant significantly increased the thermal stability of α-LA (Table I). The stabilizing effects of both mutations were easily rationalized from the electrostatic calculations in Figure 1, which showed that the carboxylate side chain of Glu1 provides distinctly unfavorable contributions; hence charge neutralization of the Glu side chain should add protein stabilization (as confirmed from the experimental data). Furthermore, electrostatic calculations for wild-type protein showed that the extra N-terminal Met residue resulted in a decrease in the favorable contributions from the positively charged α-amino group (Figure 1). Hence substantial destabilization is caused by moving the N-terminus away from a region of highly negative potential, again in accordance with experimental data (see Table I). It therefore appears that the pronounced destabilization of recombinant wild-type α-LA noted earlier is due to unfavorable charge–charge interactions.

In order to compare quantitatively the experimental data with the electrostatic calculations the mutation-induced changes in the Gibbs free energy of thermal denaturation ($\Delta\Delta G_{n\rightarrow m}$) of apo- and Ca^{2+}-loaded α-LA species were estimated from the mid-transition temperatures (t_m) in Table I. The calculations were based on DSC data for native α-LA (see Figure 3), which were analyzed according to the simple two-state model followed by calculation of the free energy change upon thermal denaturation (ΔG) according to Equation (6), given in Materials and methods:

$$\Delta\Delta G_{n\rightarrow m} = -\Delta G(t_m)$$

The resulting $\Delta\Delta G_{n\rightarrow m}$ values are presented in Table I. A comparative plot of $\Delta\Delta G_{n\rightarrow m}$ versus the change in the energy

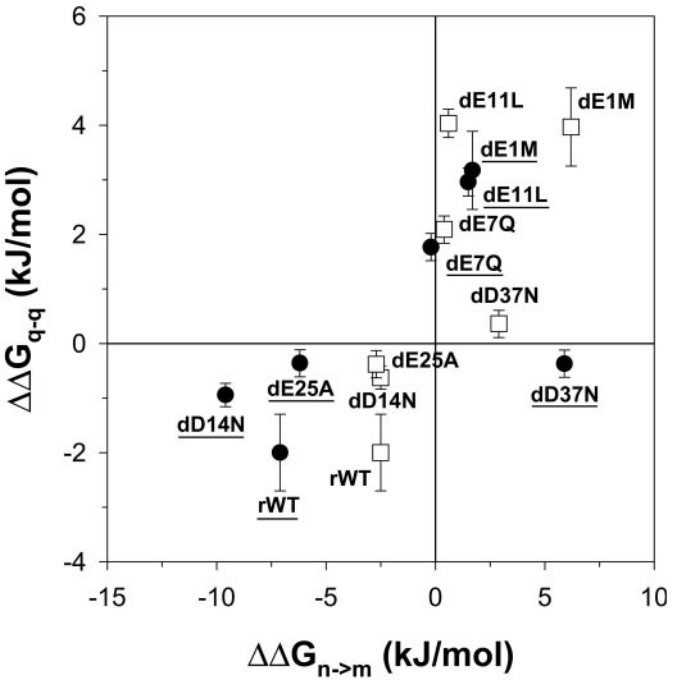

Fig. 4. Correlation between mutation-induced energy differences from experimental data ($\Delta\Delta G_{n\rightarrow m}$) and the difference in the charge–charge interactions calculated using TK-SA model ($\Delta\Delta G_{q\text{-}q}$). Open symbols are for apo form, filled symbols for Ca^{2+} form.

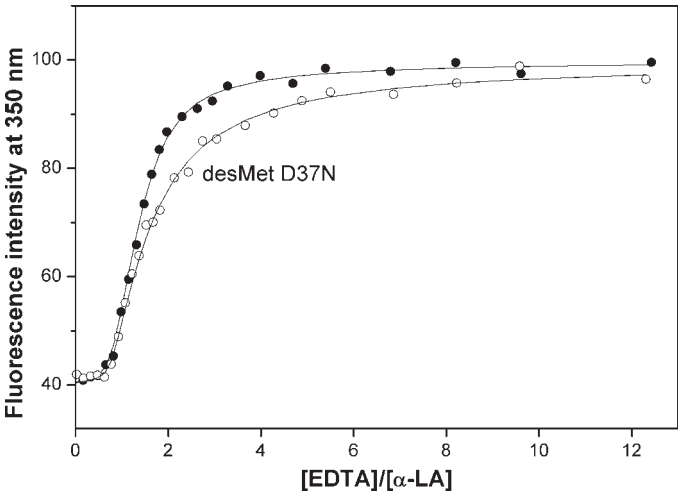

Fig. 5. Spectrofluorimetric titration of Ca^{2+}-loaded desMet D37N α-LA mutant by EDTA (10 mM HEPES–KOH, pH 7.6, 45°C) compared with the native protein. α-LA concentration was 7 μM. The excitation wavelength was 280.4 nm. Circles represent the fluorescence intensity at 350 nm in arbitrary units. The solid curves were fitted to the experimental data calculated according to the competitive binding scheme Equation 1 in Materials and methods.

of charge–charge interactions ($\Delta\Delta G_{q\text{-}q}$) is shown in Figure 4. Overall, the correlation qualitatively predicts the effects of every substitution with the possible exception of the D37N mutant. The TK-SA algorithm for this latter substitution predicted little change in stability due to changes in charge–charge interactions, whereas the experimental results showed a significant increase in stability. Since the TK-SA calculations reflect changes *only* in charge–charge interactions, other potential effects such as changes in hydrophobicity, hydrogen bonding, configurational entropy or secondary structure propensities may account for the additional stabilization.

Another distinguishing property of the studied α-LA mutants is their calcium affinity. Figure 5 depicts a typical spectrofluorimetric titration for desMet D37N α-LA. The Ca^{2+}-loaded protein was back-titrated with EDTA at 45°C (pH 7.6), which is well above the thermal transition for the apo- protein and well below the thermal transition for the Ca^{2+}-bound form (see also Figures 2 and 3). The calcium equilibrium association constants were calculated as described in Materials and methods according to Scheme (1) (Permyakov *et al*., 1985; Permyakov, 1993). Apparent calcium binding association constants for all α-LA species analyzed in this study are listed in Table I. The results show that the substitution-induced changes in calcium affinity of a given protein correlate well with concomitant changes in its thermal stability, i.e. the more thermostable mutants possess a higher affinity for Ca^{2+}. Accordingly, recombinant wild-type and desMet D14N α-LA bind Ca^{2+} about one order of magnitude weaker, whereas desMet D37N and ΔE1 α-LA bind Ca^{2+} 3–6 times more strongly than native α-LA. At 45°C, where the binding of Ca^{2+} by intact and mutant α-LA converts denatured apo-protein into native calcium-bound form (see Table I), pair-wise reduction of free energy terms corresponding to denatured apo- and calcium-saturated forms of intact and mutant proteins easily results in equality of the mutation-induced change in the free energy of denaturation of Ca^{2+}-loaded α-LA $\Delta\Delta G_{n\rightarrow m}$ and of the mutation-induced change in free energy of calcium binding (taken with the opposite sign):

$$\Delta\Delta G_{n\rightarrow m} \approx RT\ln(K_m/K_n)$$

where K_m and K_n are equilibrium calcium association constants for mutant and intact proteins, respectively. The equation above is plotted in Figure 6 for the data from Table I. The fit is certainly in qualitative agreement with the equation above. Hence the improvement in α-LA thermal stability described here is related to an enhancement of calcium binding affinity.

Role of charge–charge interactions in structural stabilization

Computational analysis of charge–charge interactions in bovine α-LA conducted in this work was qualitatively validated by experiment. The N-terminal sequence (residues 1–11) is characterized by a high proportion of negatively charged residues that cluster on the surface of the native protein. Neutralization of unfavorable charge–charge interactions in the N-terminus results in stabilization of both the apo- and Ca^{2+}-bound protein. As also demonstrated above, an increase in thermal stability is related to an increase in calcium binding affinity. If one considers the binding of basic proteins, histones or positively charged polyamino acids, these interactions are accompanied by different effects (Permyakov *et al*., 2004). Although the interaction with basic polymers increased the thermal stability of apo-α-LA, the calcium-saturated protein was *destabilized* (the calcium affinity was diminished also). An example that illustrates the comparable mechanism is the effect of Asp87 replacement, which directly coordinates the calcium ion in α-LA, with the neutral side chain Asn (Permyakov *et al*., 2001). The resulting decrease in calcium binding affinity was about two orders of magnitude with an accompanying decrease in thermal stability of the Ca^{2+}-loaded protein. It is likely that the same destabilization of the Ca^{2+}-saturated form occurs in the case of α-LA interactions with the basic proteins,

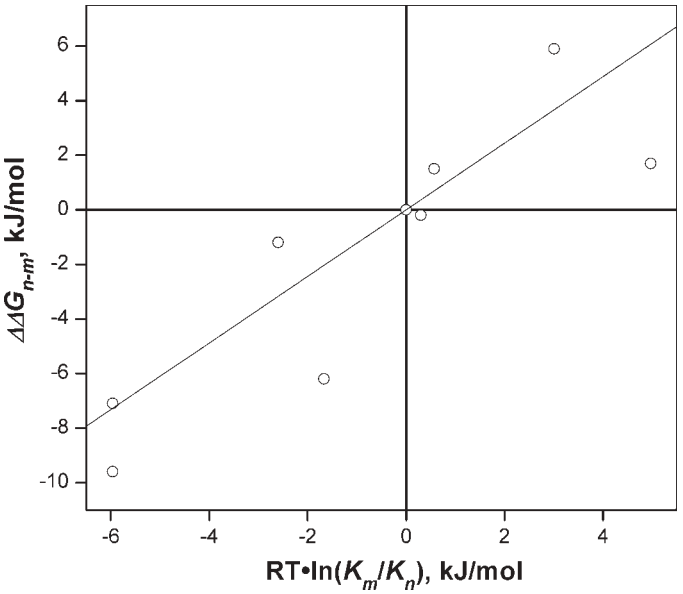

Fig. 6. Correlation between mutation-induced changes in free energy of thermal denaturation ($\Delta\Delta G_{n\rightarrow m}$) of Ca^{2+}-loaded α-LA and the free energy of calcium binding [$RT\ln(K_n/K_m)$], where K_m and K_n are equilibrium calcium association constants for mutant and intact proteins, respectively). Data are taken from Table I.

i.e. involvement of the highly negatively charged calcium-binding loop in the binding of basic proteins results in a decrease in calcium affinity, consequently decreasing the thermal stability of the Ca^{2+}-loaded protein. The interaction of apo-protein with a basic polymer stabilizes α-LA via the neutralization of the highly unfavorable negative charge distribution of the calcium binding-loop (see Figure 1). Hence the N-terminus may be involved in similar compensating interactions with histones, positively charged polyamino acids and other polycations *in vivo*.

It should be noted that, despite many years of protein engineering studies with α-LA, rarely have mutations been found that improve protein physico-chemical properties. We are aware of only two cases where a significant increase in α-LA thermal stability was found and most of these mutations were not planned via rational computational approaches (Greene *et al*., 1999; Veprintsev *et al*., 1999). This strategy was first proposed by Loladze *et al*. in 1999 (Loladze *et al*., 1999) based on experimental data from several papers, which showed that mutations in surface charges can significantly alter protein stability (Grimsley *et al*., 1999; Paoli *et al*., 1999; Perl *et al*., 2000; Spector *et al*., 2000). It was further reinforced when it was shown that computational approaches are capable of qualitatively predicting the consequences of surface charge mutations on protein stability (Perl and Schmid, 2001; Sanchez-Ruiz and Makhatadze, 2001; Forsyth *et al*., 2002; Zhou, 2002b; Luisi *et al*., 2003; Makhatadze *et al*., 2003; Schwehm *et al*., 2003).

The results presented here provide experimental validation for rational optimization of charge–charge interactions on a protein surface as a tool to modulate protein stability. Examination of the energy contributed by Glu1 and the energetically favorable consequences of neutralizing this residue clearly suggests that nature may have made an error with bovine α-LA (as opposed to the human and most other species, which contain an N-terminal Lys!). Or was this destabilizing contribution intentional for other physiological reasons? Further studies on the differences between bovine and other α-LA species in physiological function may shed more light on this question.

Acknowledgements

We acknowledge Takuji Kobayashi and Richard Kristinsson for their technical assistance. This work was supported in part by grants from the USPHS (NIH GM 56970 to L.J.B.), the National Science Foundation (MCB-0110396 to G.I.M.), the Programs of the Russian Academy of Sciences ('Fundamental science for medicine' and 'Molecular and cellular biology'), a grant of the Russian Fund for Basic Research (04-04-97322 to E.A.P.) and INTAS (01-2347 CA to V.N.U., E.A.P. and S.E.P.).

References

Anderson,P.J., Brooks,C.L. and Berliner,L.J. (1997) *Biochemistry*, **36**, 11648–11654.
Antosiewicz,J., McCammon,J.A. and Gilson,M.K. (1994) *J. Mol. Biol.*, **238**, 415–436.
Aramini,J.M., Drakenberg,T., Hiraoki,T., Ke,Y., Nitta,K. and Vogel,H.J. (1992) *Biochemistry*, **31**, 6761–6768.
Bashford,D. (2004) *Front. Biosci.*, **9**, 1082–1099.
Bismuto,E., Febbraio,F., Limongelli,S., Briante,R. and Nucci,R. (2003) *Proteins*, **51**, 10–20.
Bjork,A., Dalhus,B., Mantzilas,D., Sirevag,R. and Eijsink,V.G. (2004) *J. Mol. Biol.*, **341**, 1215–1226.
Burstein,E.A. and Emelyanenko,V.I. (1996) *Photochem. Photobiol.*, **64**, 316–320.
Chaudhuri,T.K. *et al*. (1999) *J. Mol. Biol.*, **285**, 1179–1194.
Chen,J., Lu,Z., Sakon,J. and Stites,W.E. (2000) *J. Mol. Biol.*, **303**, 125–130.
Chrysina,E.D., Brew,K. and Acharya,K.R. (2000) *J. Biol. Chem.*, **275**, 37021–37029.
Dolgikh,D.A., Gilmanshin,R.I., Brazhnikov,E.V., Bychkova,V.E., Semisotnov,G.V., Venyaminov,S. and Ptitsyn,O.B. (1981) *FEBS Lett.*, **136**, 311–315.
Dominy,B.N., Minoux,H. and Brooks,C.L.,III (2004) *Proteins*, **57**, 128–141.
Dong,F. and Zhou,H.X. (2002) *Biophys. J.*, **83**, 1341–1347.
Duringer,C., Hamiche,A., Gustafsson,L., Kimura,H. and Svanborg,C. (2003) *J. Biol. Chem.*, **278**, 42131–42135.
Elcock,A.H. and McCammon,J.A. (1998) *J. Mol. Biol.*, **280**, 731–748.
Feig,M., Onufriev,A., Lee,M.S., Im,W., Case,D.A. and Brooks,C.L.,III (2004) *J. Comput. Chem.*, **25**, 265–284.
Fitch,C.A., Karp,D.A., Lee,K.K., Stites,W.E., Lattman,E.E. and Garcia-Moreno,E.B. (2002) *Biophys, J.,* **82**, 3289–3304.
Forsyth,W.R., Antosiewicz,J.M. and Robertson,A.D. (2002) *Proteins*, **48**, 388–403.
Garcia-Moreno,E.B. and Fitch,C.A. (2004) *Methods Enzymol.*, **380**, 20–51.
Gilson,M.K. (1995) *Curr. Opin. Struct. Biol.*, **5**, 216–223.
Greene,L.H., Grobler,J.A., Malinovskii,V.A., Tian,J., Acharya,K.R. and Brew,K. (1999) *Protein Eng.*, **12**, 581–587.
Grimsley,G.R., Shaw,K.L., Fee,L.R., Alston,R.W., Huyghues-Despointes,B.M., Thurlkill,R.L., Scholtz,J.M. and Pace,C.N. (1999) *Protein Sci.*, **8**, 1843–1849.
Guerois,R., Nielsen,J.E. and Serrano,L. (2002) *J. Mol. Biol.*, **320**, 369–387.
Hackel,M., Hinz,H.J. and Hedwig,G.R. (1999) *J. Mol. Biol.*, **291**, 197–213.
Hakansson,A., Zhivotovsky,B., Orrenius,S., Sabharwal,H. and Svanborg,C. (1995) *Proc. Natl Acad. Sci. USA*, **92**, 8064–8068.
Hakansson,A., Andreasson,J., Zhivotovsky,B., Karpman,D., Orrenius,S. and Svanborg,C. (1999) *Exp. Cell Res.*, **246**, 451–460.
Ibarra-Molero,B., Loladze,V.V., Makhatadze,G.I. and Sanchez-Ruiz,J.M. (1999) *Biochemistry*, **38**, 8138–8149.
Ishikawa,N., Chiba,T., Chen,L.T., Shimizu,A., Ikeguchi,M. and Sugai,S. (1998) *Protein Eng.*, **11**, 333–335.
Klapper,I., Hagstrom,R., Fine,R., Sharp,K. and Honig,B. (1986) *Proteins*, **1**, 47–59.
Kronman,M.J. Aandreotti,R. and Vitols,R. (1964) *Biochemistry*, **28**, 1152–1160.
Kunkel,T.A. (1985) *Proc. Natl Acad. Sci. USA*, **82**, 488–492.
Loladze,V.V., Ibarra-Molero,B., Sanchez-Ruiz,J.M. and Makhatadze,G.I. (1999) *Biochemistry*, **38**, 16419–16423.
Luisi,D.L., Snow,C.D., Lin,J.J., Hendsch,Z.S., Tidor,B. and Raleigh,D.P. (2003) *Biochemistry*, **42**, 7050–7060.
Makhatadze,G.I., Loladze,V.V., Ermolenko,D.N., Chen,X. and Thomas,S.T. (2003) *J. Mol. Biol.*, **327**, 1135–1148.

Makhatadze,G.I., Loladze,V.V., Gribenko,A.V. and Lopez,M.M. (2004) *J. Mol. Biol.*, **336**, 929–942.
Marquardt,D.W. (1963) *J. Soc. Ind. Appl. Math.*, **11**, 431–441.
Matthew,J.B. and Gurd,F.R. (1986) *Methods Enzymol.*, **130**, 413–436.
Minagawa,H., Shimada,J. and Kaneko,H. (2003) *Eur. J. Biochem.*, **270**, 3628–3633.
Mozo-Villarias,A., Cedano,J. and Querol,E. (2003) *Protein Eng.*, **16**, 279–286.
Paoli,P., Taddei,N., Fiaschi,T., Veggi,D., Camici,G., Manao,G., Raugei,G., Chiti,F. and Ramponi,G. (1999) *Arch. Biochem. Biophys.*, **363**, 349–355.
Pellegrini,A., Thomas,U., Bramaz,N., Hunziker,P. and von Fellenberg,R. (1999) *Biochim. Biophys. Acta*, **1426**, 439–448.
Perl,D. and Schmid,F.X. (2001) *J. Mol. Biol.*, **313**, 343–357.
Perl,D., Mueller,U., Heinemann,U. and Schmid,F.X. (2000) *Nat. Struct. Biol.*, **7**, 380–383.
Permyakov,E.A. (1993) *Luminescent Spectroscopy of Proteins*. CRC Press, Boca Raton, FL.
Permyakov,E.A. and Berliner,L.J. (2000) *FEBS Lett.*, **473**, 269–274.
Permyakov,E.A. and Burstein,E.A. (1984) *Biophys. Chem.*, **19**, 265–271.
Permyakov,E.A., Burstein,E.A., Sawada,Y. and Yamazaki,I. (1977) *Biochim. Biophys. Acta*, **491**, 149–154.
Permyakov,E.A., Morozova,L.A. and Burstein,E.A. (1985) *Biophys. Chem.*, **21**, 21–31.
Permyakov,E.A., Murakami,K. and Berliner,L.J. (1987) *J. Biol. Chem.*, **262**, 3196–3198.
Permyakov,E.A., Permyakov,S.E., Deikus,G.Y., Morozova-Roche,L.A., Grishchenko,V.M., Kalinichenko,L.P. and Uversky,V.N. (2003) *Proteins*, **51**, 498–503.
Permyakov,S.E., Veprintsev,D.B., Brooks,C.L., Permyakov,E.A. and Berliner,L.J. (2000) *Proteins*, **40**, 106–111.
Permyakov,S.E., Uversky,V.N., Veprintsev,D.B., Cherskaya,A.M., Brooks,C.L., Permyakov,E.A. and Berliner,L.J. (2001) *Protein Eng.*, **14**, 785–789.
Permyakov,S.E., Pershikova,I.V., Khokhlova,T.I., Uversky,V.N. and Permyakov,E.A. (2004) *Biochemistry*, **43**, 5575–5582.
Prescott,J.M. and Wilkes,S.H. (1976) *Methods Enzymol.*, **45**, 530–543.
Privalov,P.L. and Potekhin,S.A. (1986) *Methods Enzymol.*, **131**, 4–51.
Sanchez-Ruiz,J.M. and Makhatadze,G.I. (2001) *Trends Biotechnol.*, **19**, 132–135.
Schaefer,M., van Vlijmen,H.W. and Karplus,M. (1998) *Adv. Protein Chem.*, **51**, 1–57.
Schutz,C.N. and Warshel,A. (2001) *Proteins*, **44**, 400–417.
Schwarzenbach,G. and Flaschka,H. (1965) *Die Komplexometrische Titration*. Ferdinand Enke Verlag, Stuttgart.
Schwehm,J.M., Fitch,C.A., Dang,B.N., Garcia-Moreno,E.B. and Stites,W.E. (2003) *Biochemistry*, **42**, 1118–1128.
Spector,S., Wang,M., Carp,S.A., Robblee,J., Hendsch,Z.S., Fairman,R., Tidor,B. and Raleigh,D.P. (2000) *Biochemistry*, **39**, 872–879.
Svensson,M., Sabharwal,H., Hakansson,A., Mossberg,A.K., Lipniunas,P., Leffler,H., Svanborg,C. and Linse,S. (1999) *J. Biol. Chem.*, **274**, 6388–6396.
Svensson,M., Hakansson,A., Mossberg,A.K., Linse,S. and Svanborg,C. (2000) *Proc. Natl Acad. Sci. USA*, **97**, 4221–4226.
Tanford,C. and Kirkwood,J.G. (1957) *J. Am. Chem. Soc.*, **79**, 5333–5339.
Vanhooren,A., Devreese,B., Vanhee,K., Van Beeumen,J. and Hanssens,I. (2002) *Biochemistry*, **41**, 11035–11043.
Veprintsev,D.B., Permyakov,S.E., Permyakov,E.A., Rogov,V.V., Cawthern,K.M. and Berliner,L.J. (1997) *FEBS Lett.*, **412**, 625–628.
Veprintsev,D.B., Narayan,M., Permyakov,S.E., Uversky,V.N., Brooks,C.L., Cherskaya,A.M., Permyakov,E.A. and Berliner,L.J. (1999) *Proteins*, **37**, 65–72.
Wilkes,S.H., Bayliss,M.E. and Prescott,J.M. (1973) *Eur. J. Biochem.*, **34**, 459–466.
Zhou,H.X. (2002a) *Proc. Natl Acad. Sci. USA*, **99**, 3569–3574.
Zhou,H.X. (2002b) *Biochemistry*, **41**, 6533–6538.

Received April 5, 2005; revised June 28, 2005; accepted June 30, 2005

Edited by Gideon Schreiber